

Estimation of snow depth and detection of buried objects using airborne Ground Penetrating Radar in Indian Himalaya

H. S. Negi*, Snehmani, N. K. Thakur and J. K. Sharma

Snow and Avalanche Study Establishment, Chandigarh 160 036, India

The aim of this study has been to explore the utility of airborne Ground Penetrating Radar (GPR) in rugged mountainous region, for the estimation of snow depth profile and detection of buried objects in the snow cover. After conducting the airborne GPR survey, the results obtained for snow depth and detection of buried objects were found to be in good agreement with the ground observations. These results would be helpful in providing important inputs in the future for better planning, execution and exploitation of airborne GPR survey technology for detailed study of snow-covered and glaciated remote areas of the Indian Himalaya.

Keywords: Airborne ground penetrating radar, buried objects, dielectric constant, snow depth.

LARGE areas in the Himalayas are covered with seasonal snow during winter and significant changes occur in the snow cover during summer. Changes in snow depth influence hydropower generation, water management, mass-balance study, strategic planning, avalanche forecasting, flood forecasting and other developmental activities, which contribute to the national economy. This necessitates efficient estimation of snow depth over the rugged mountainous terrain for planning and management of the above-mentioned activities.

Estimation of snow depth in the snow-bound, inaccessible Himalayan regions using ground-based conventional techniques is difficult, time-consuming and area-specific only. The Ground Penetrating Radar (GPR) offers a faster and non-destructive alternative to conventional snow surveys, by providing a continuous profile of the large areas and signatures of buried objects quickly¹. GPR uses electromagnetic (EM) radiation in the microwave frequency range between 10 and 1000 MHz for a number of applications, including in the cold regions because of the excellent penetration of EM waves in snow and ice.

The ground-based GPR is extensively used world over for snow-related studies, but its use in airborne mode has not been much reported. Some GPR-based snow/glacier case studies have been reported from Antarctica, Arctic

and other countries as well²⁻⁷. However, in the Indian context, this area remains quite unexplored. Some ground-based GPR studies have been carried out in the Indian Himalaya for measurement of snow depth, avalanche debris, detection of buried objects and crevasses, but several practical difficulties have been reported in carrying out such ground surveys^{8,9}. Therefore, the airborne GPR survey was carried out to overcome some of these difficulties and also to check its utility for such studies.

Study area

The study sites selected are two snow-meteorological observatories in field near HQ Snow and Avalanche Study Establishment (SASE), Manali; Patsio (in the Greater Himalayan Range) referred to as location-A and Dhundi (in Pir Panjal Range) referred to as location-B of the Indian Himalaya. The Pir Panjal Range (Lower Himalayan zone) is characterized by its warm temperature and high precipitation rate¹⁰. Due to prevalence of warmer temperatures, the snow cover changes quickly into isothermal snow pack at 0°C. The average altitude of the Pir Panjal Range lies between 2000 and 4000 m. The Greater Himalayan Range (Middle Himalayan zone) is characterized by cold temperature and receives dry snowfall. Altitude of this range varies from 3500 to 5300 m. The extent of existing snow cover in the study area is shown in IRS-P6/Resourcesat satellite imagery of 12 March 2006 (FCC: 2, 3, 5; Figure 1). The airborne GPR survey was carried out on 12 March 2006 at location-A and on 13 March 2006 at location-B.

For survey location-A, the survey area was bounded by the following latitudes and longitudes:

- DF01: N32.75322–E077.26222
- DF02: N32.75316–E077.26247
- DF03: N32.75299–E077.26245
- DF04: N32.75290–E077.26251
- DF05: N32.75271–E077.26255
- DF06: N32.75268–E077.26244
- DF07: N32.75303–E077.26222

For survey location-B, the survey area was bounded by the following latitudes and longitudes:

*For correspondence. (e-mail: negi_hs@yahoo.com)

- DF01: N32.35536–E077.12512
- DF02: N32.35547–E077.12484
- DF03: N32.35551–E077.12454
- DF04: N32.35530–E077.12454
- DF05: N32.35521–E077.12471
- DF06: N32.35516–E077.12507
- DF07: N32.35514–E077.12539

Instruments used and methodology

Airborne GPR survey details

The Hemispherical Butterfly Dipole (HBD-350) GPR antenna (Radarteam, Sweden) was used for the airborne survey. It is top shielded and well suited for snow thickness measurements from airborne platforms such as helicopters (Figure 2). The SIR-3000 digital Subsurface Interface Radar (SIR) System was used to collect and record data from the survey sites. The raw data were trans-

ferred to a recording device (laptop) for further processing. The data collected from both survey sites were processed with COBRA Post Processing software (ver. 7.03). M-Master software (Radarteam) was used to generate accurate marker positions which allow the operator to specify space intervals and send marker positions to the SIR-3000 collection system. The markers were then superimposed with the raw data to find the spatial components of the buried objects. The flight data and the track log were also recorded using GPS (Garmin Rino 130), with a digital altimeter to provide accurate records for analysis.

For survey location-A, the flying height of the helicopter was between 3793 and 3804 m asl. The total area covered

Table 1. GPR survey parameters at locations A and B

| Survey parameter | Location-A | Location-B |
|---|------------|------------|
| Peak frequency (MHz) | 342 | 342 |
| Centre frequency (BW _{10dB} ; MHz) | 334 | 334 |
| Distance between the TX/RX terminals (mm) | 345 | 345 |
| Samples per scan | 512 | 512 |
| Bits per data | 8 | 8 |
| Scans/s | 30 | 64 |
| Scans/m | 40 | 40 |
| Time window/range (ns) | 120 | 60 |
| Number of scans | 8320 | 5424 |
| Number of channels | 1 | 1 |
| Total distance covered (m) | 205 | 135.50 |
| Speed of helicopter during survey (kmph) | 64 | 21 |

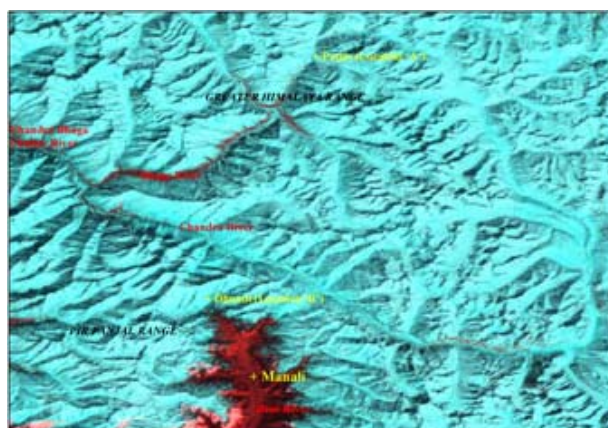


Figure 1. IRS-P6 imagery (12 March 2006) showing snow cover extent in the study area and survey locations.



Figure 2. Helicopter-based airborne GPR survey of the study area using HBD-350 antenna.

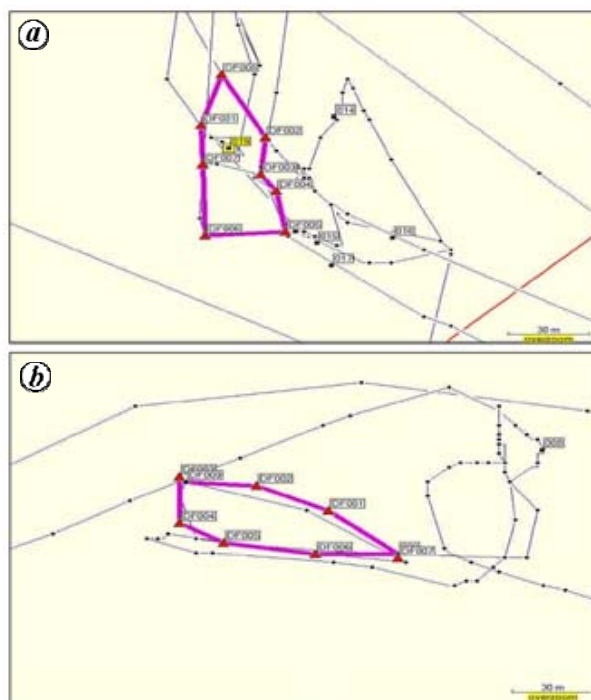


Figure 3. Track log of helicopter at (a) survey location-A and (b) survey location-B.



Figure 4. Positioning of planted objects at both the survey locations before onset of winter.

Table 2. Snow pit data observations at survey location-A

| Layer no. | Layer thickness (cm) | Wetness | Density (g/cc) |
|-----------|----------------------|---------|----------------|
| 1 | 4 | Dry | 0.28 |
| 2 | 13 | Dry | 0.27 |
| 3 | 6 | Dry | 0.3 |
| 4 | 6 | Dry | 0.4 |
| 5 | 7 | Dry | 0.32 |
| 6 | 4 | Dry | – |
| 7 | 6 | Dry | 0.32 |
| 8 | 1 | Dry | – |
| 9 | 49 | Dry | 0.44 |
| 10 | 23 | Dry | 0.44 |
| 11 | 10 | Dry | 0.47 |
| 12 | 8 | Dry | 0.4 |

during the survey was approximately 1708 sq. m in a single pass (Figure 3a). A trace was acquired at every 0.025 m. For survey location-B, the flying height of the helicopter was between 2856 and 2886 m asl. The length of the time window depends on the desired depth of investigation and the velocity of the radar wave in the ground. For very shallow investigations, it may be useful to decrease the default time window to increase the system performance. As the snow thickness was less at location-B, the time window was reduced to 60 ns and the number of scans increased to 64/s. Helicopter speed was reduced to approximately 20 kmph. The total area covered during the survey was approximately 1797 sq. m (Figure 3b). The other GPR survey parameters are given in Table 1.

Ground observations

The snow stratigraphy data were collected at location-A during survey (Table 2). The total snow thickness at the observatory location was 137 cm and the average snow density was 0.36 g/cc. At location-B, the snow pack was isotherm due to warm temperatures in March at the

Lower Himalayan zone. Therefore, the complete snow pack of 50 cm depth was isotherm, having wet snow of density 0.34 g/cc. For the study of buried objects, three rows of objects (barrels of 55 cm dia and 90 cm length) were planted on the ground before the onset of winter (Figure 4). The first row was kept vertical on the ground, the second row was laid at 8 m distance and the third row was laid at a distance of 4 m from the second row.

Snow depth estimation

Depth measurement depends on dielectric constant (ϵ_r) of the medium^{11,12}. The dielectric properties of snow usually divide it into two phases: (a) dry snow, which is a mixture of ice and air and contains no free (liquid) water, and (b) wet snow, which contains free water. In the present study, few snow parameters were collected e.g. snow density, type of snow, etc. Using these parameters, the value of dielectric constant was estimated. The following relations were used for dry snow studies¹³:

$$\epsilon'_{ds} = 1.0 + 1.83\rho \quad \text{for } \rho \leq 0.5 \text{ g/cm}^3, \text{ and}$$

$$\epsilon'_{ds} = 0.51 + 2.88\rho \quad \text{for } \rho \geq 0.5 \text{ g/cm}^3. \quad (1)$$

For wet-snow studies, Polder-Van Santen had developed the following empirical expressions from the experimental measurements¹⁴:

$$\epsilon'_{ds} = 1.0 + 2.2\rho, \quad (2)$$

$$\epsilon'_{ws} = \epsilon'_{ds} + 0.213m_v (\%), \quad (3)$$

where ϵ'_{ds} and ϵ'_{ws} are the dielectric constants of dry and wet snow respectively, ρ the density of snow (g/cc) and m_v (%) is the volume fraction of liquid water expressed as a percentage.

For depth/height measurements of the medium, the velocity of the EM wave in the medium has to be estimated. The velocity of the radar wave in the material varies with

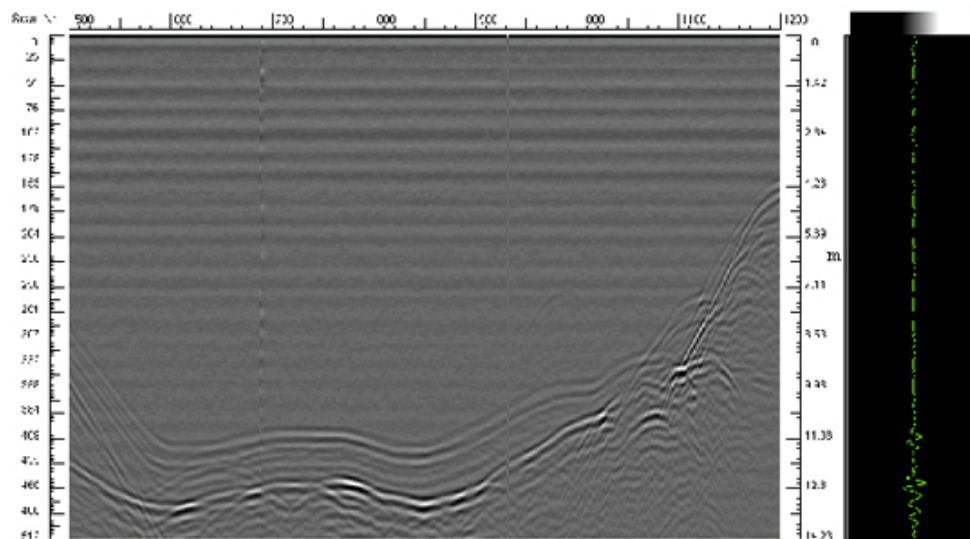


Figure 5. GPR profile of snow thickness at SASE field observatory in location-A (radargram and trace window).

the dielectric constant of the medium¹¹. The velocity (v) at which the EM wave travels through the medium is given by:

$$v = c/(\epsilon_r)^{1/2}, \quad (4)$$

where c is the speed of light (3×10^8 m/s).

Results and discussion

The airborne GPR survey data (radargrams) were analysed with COBRA Post Processing Software (ver. 7.03). Some GPR data loss was observed at a few points acquired over the survey location-A, which may be due to difficulty in maintaining a constant flying height of the helicopter over the rugged mountainous area, non-availability of accurate altimeter in the helicopter and lack of audible communication between the surveyor and the pilot. The variable altitude of the helicopter (40–50 m) provided sub-surface signatures out of the time-window range. Mal-functioning of the GPS failed to provide markers at location-A. However, the flight data and the track log were also recorded with GPS (Garmin Rino 130) during the survey. Positioning in the radargram was done using this GPS and the snow profile was identified. Different filtering processes were applied to remove the unwanted disturbances and enhance the desired features using post-processing software.

The average density of snow at location A was estimated as 0.36 g/cc (Table 2). As the snow was dry, applying eq. (6), a dielectric constant of 1.66 was obtained. Hence, the estimated value of the EM wave velocity in the medium was 230 m/ μ s (eq. (4)). The radargram of

snow depth at location-A is shown in Figure 5. Snow and ground interface can clearly be distinguished in the radargram due to strong reflections. Simultaneously, the trace window on the right side shows the amplitudes corresponding to air–snow and snow–soil interface distances, i.e. 140 cm, which is equivalent to snow thickness. This is in good agreement with actual snow depth of 137 cm observed at the ground (Table 2). The estimated total volume of snow in the survey location-A was found to be 2391 m³.

Snow thickness along a north-facing left-side slope was observed to be 140 cm, whereas the right-side south-facing slope was snow-free (Figure 6). Strong reflection was observed at the valley/channel, which may be due to presence of water at the bottom of the snow cover, as there is strong dielectric contrast between snow and water. The signatures of buried objects could not be identified during the survey at location-A, which may be because of the large time window (120 ns), high speed (64 kmph) and flying height of the helicopter, or the size of the buried objects being less than the GPR frequency.

Therefore, the experiments were carried out with modified survey parameters at location-B, as shown in Table 1. The density of the snow at location-B was 0.34 g/cc. Since the snow was wet, applying eqs (2) and (3), the dielectric constant was found to be 2.38, and the estimated value of the EM wave velocity in the medium was 194 m/ μ s. The average snow depth was estimated as 55 cm at location-B. The radargram of snow depth (Figure 7) also showed the presence of buried objects (hyperbolic signatures) in the snow cover. The marker data at 1 m interval were laid on the radargram. At 80 m marking distance, the first signature of buried objects was observed, corresponding to row-1 (Figure 4, location-B). Another weak signature of

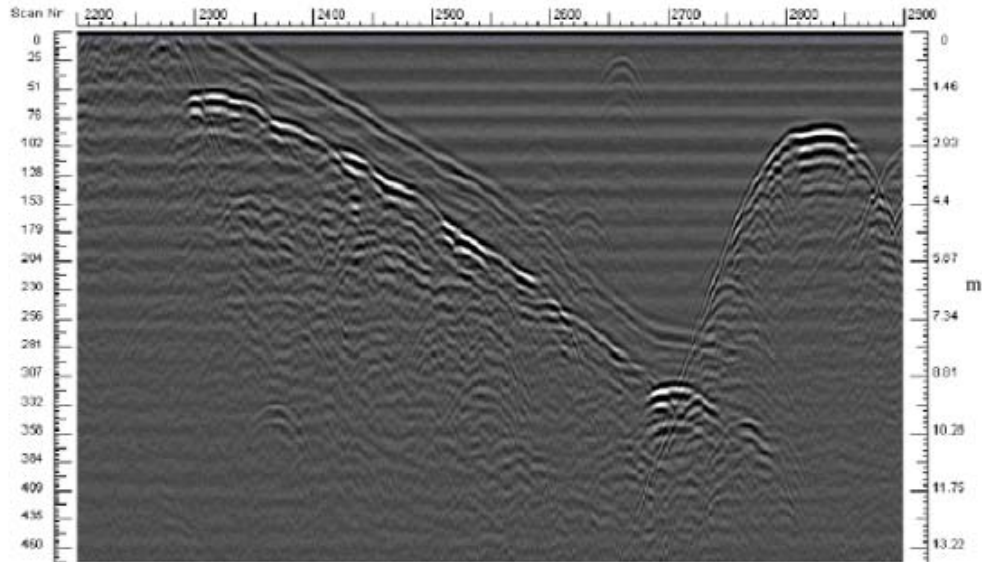


Figure 6. GPR profile of snow thickness along north and south-facing slopes at location-A.

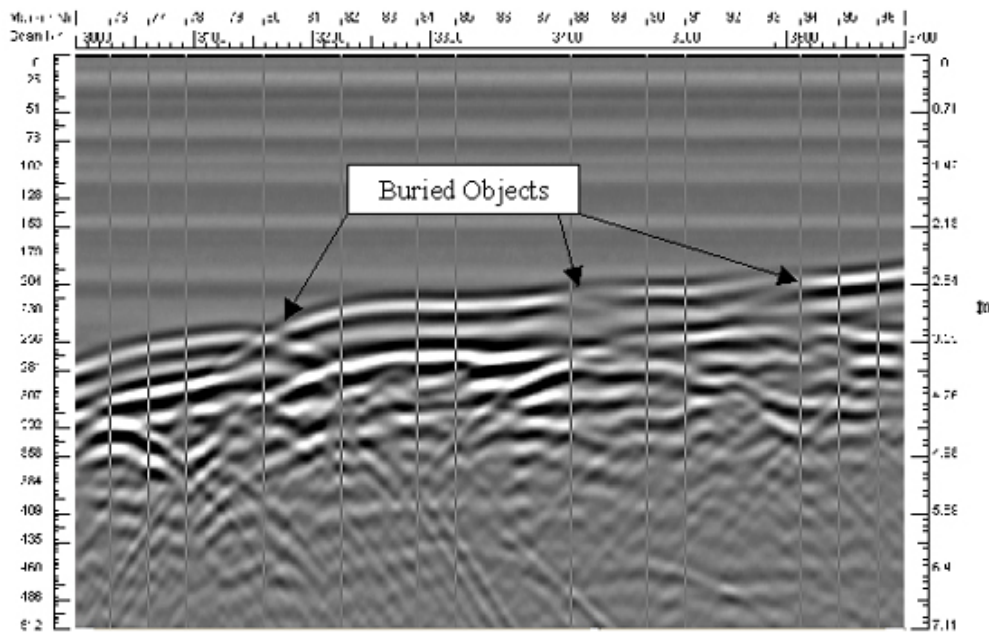


Figure 7. GPR signatures of buried objects at survey location-B.

buried objects was observed at 88 m distance, which showed good agreement of 8 m interval with the initial ground observation (row-2). The third weak signature of buried objects was observed at 93 m marking distance, which showed 5 m interval between rows 2 and 3. Thus, the results obtained for buried objects are approximately at the same interval as in the ground.

Conclusion

From the airborne GPR data acquired over location-A, the average thickness of the snow was 140 cm and the total volume of snow was 2391 m³. For location-B, the average thickness of snow in the surveyed area was 55 cm and the total volume of snow was 988 m³. These results were

found to be in reasonable agreement with the ground observations. The airborne GPR was able to determine the depth of buried objects in snow cover and the distance between these objects with good accuracy.

By virtue of the excellent penetration of radar waves in snow pack, airborne GPR offers a quick and efficient tool for snow and glacier-related studies. The present study has provided vital inputs for better planning and execution of future airborne GPR surveys in the Himalayan region. Though there are certain constraints, by conducting more such trials this technology can be exploited suitably for snow and glacier-related studies.

1. Jaedicke, C., Snow mass quantification and avalanche victim search by ground penetrating radar. *Surv. Geophys.*, 2003, **24**, 431–445.
2. Anna, S., Aslak, G., John, C. M., Eija, K. and Rickard, P., Snow-accumulation studies in Antarctica with ground-penetrating radar using 50, 100 and 800 MHz antenna frequencies. *Ann. Glaciol.*, 2003, **37**, 194–198.
3. Tabacco, I. E., Bianchi, C., Irizzotti, A., Zuccheretti, E., Forieri, A. and Dellavedova, A., Airborne radar survey above Vostok region, east-central Antarctica: Ice thickness and Lake Vostok geometry. *J. Glaciol.*, 2002, **48**, 62–69.
4. Arcone, S. A., Airborne-radar stratigraphy and electrical structure of temperate firn: Bagley Ice Field, Alaska, USA. *J. Glaciol.*, 2002, **48**, 317–334.
5. Kennett, M., Laumann, T. and Lund, C., Helicopter-borne radio-echo sounding of Svartisen, Norway. *Ann. Glaciol.*, 1993, **17**, 23–26.
6. Jacobel, R. W. and Bindschadler, R., Radar studies at the mouths of ice streams D and E, Antarctica. *Ann. Glaciol.*, 1993, **17**, 262–268.
7. Palli, A., Kohler, J. C., Isaksson, E., Moore, J. C., Pinglot, J. F., Pohjola, V. A. and Samuelsson, H., Spatial and temporal variability of snow accumulation using ground-penetrating radar and ice cores on a Svalbard glacier. *J. Glaciol.*, 2002, **48**, 417–424.
8. Negi, H. S., Mishra, V. D., Singh, K. K. and Mathur, P., Application of ground penetrating radar for snow, ice and glacier studies. In Proceedings of the International Symposium on Snow Monitoring and Avalanches, SASE Manali, 12–16 April 2004.
9. Negi, H. S., Singh, K. K., Mishra, V. D., Thakur, N. K. and Mathur, P., Depth measurements using Ground Penetrating Radar in NW-Himalayan region. In Proceedings of the Second International Symposium on Microwaves, Antenna, Propagation and Remote Sensing, ICRS Jodhpur, 23–25 November 2004.
10. Sharma, S. S. and Ganju, A., Complexities of avalanche forecasting in Western Himalaya – An overview. *Cold Regions Sci. Technol.*, 2000, **31**, 95–102.
11. Annan, A. P., Ground penetrating radar: Workshop notes, Sensors and Software, Inc., Mississauga, Ontario, 1996, p. 106.
12. Ulaby, F. T., Bengal, T., Dobson, M. C., East, J. R., Garvin, J. B. and Evans, D. L., Microelectric dielectric properties of dry rocks. *IEEE Trans. Geosci. Remote Sensing*, 1990, **28**, 325–336.
13. Hallikainen, M., Ulaby, F. T. and Abdelrazik, M., The dielectric behavior of snow in the 3- to 37-GHz range. In Proceedings of the IGARSS Symposium, Strasbourg, 27–30 August 1984.
14. Ulaby, F. T., Moore, R. K. and Fung, A. K., Microwave remote sensing active and passive. Vol. III, Artech House, Norwood MA, 1986, p. 2069.

ACKNOWLEDGEMENTS. We are grateful to Dr R. N. Sarwade, Director, SASE, Chandigarh for constant motivation and support to make these trials feasible.

Received 8 August 2007; revised accepted 6 February 2008